Bulletin of the New Zealand Society for Earthquake Engineering, Vol. 59, No. 1, March 2026

EVALUATING THE DISPLACEMENT CAPACITY OF SLENDER RECTANGULAR REINFORCED CONCRETE WALLS USING MOMENT-CURVATURE ANALYSIS

Arsalan Niroomandi[1], Mahshid Firoozbakhtian[2], Mohammad Amir Najafgholipour[3], Timothy J. Sullivan[4] and Craig Stevenson[5]

(Submitted *August 2024*; Reviewed *January 2025*; Accepted *June 2025*)

ABSTRACT

To aid with seismic design and assessment, the force-displacement capacity of a structural wall is commonly determined by evaluating a total rotation capacity comprising elastic and plastic deformation components, utilising a moment-curvature section analysis approach. The plastic rotation capacity is dependent on the adopted equivalent plastic hinge length. Although numerous equations for determining the plastic hinge length of slender walls are documented in the literature, their precision remains uncertain. This research collected a database of slender reinforced concrete wall specimens that demonstrated flexural failure modes, in order to evaluate the accuracy of the moment curvature method. For this purpose, the observed drift capacity is compared with the drift capacity estimated using commonly referred to equations for the plastic hinge length of reinforced concrete walls and subsequently, a new plastic hinge length expression is proposed to improve accuracy and reduce variability in predictions. Moreover, the displacement capacities of slender walls calculated using the moment-curvature method are contrasted with results from a direct rotation approach. (based on EN1998-03, ASCE 41-17, and ACI 369-22). The moment-curvature method aligns more closely with the experimental data compared to the direct rotation method and offers additional insights into the seismic performance of slender walls.

https://doi.org/10.5459/bnzsee.1714

INTRODUCTION

Reinforced concrete (RC) walls are widely used as primary lateral load resisting elements of structures to resist seismic actions. Based on the ratio of height to length, the walls can be categorized as either squat or slender. The seismic response of squat walls, which typically have a height to length ratio less than one, is primarily influenced by shear deformations, leading to diverse shear failure modes including diagonal compression/web crushing, diagonal tension, and sliding shear [1]. For slender walls, where the height to length ratios exceed two, the seismic behaviour is generally controlled by flexural deformations.

Drawing from documented damage in buildings from past earthquakes [2-7] and experimental research [8-17], slender walls may exhibit diverse failure mechanisms. These include flexural yielding due to the yielding of longitudinal reinforcement (Figure 1a), concrete crushing, reinforcement bar buckling, diagonal tension (Figure 1b) and compression, sliding shear at the construction joints (Figure 1c), hinge sliding (Figure 1d), behaviour consistent with a single crack [18], lateral instability (Figure 1e), and out-of-plane shear-axial failures [19,20].

Understanding the seismic behaviour of structural systems requires accurate assessment of the deformation capacity of their individual elements. In the case of RC walls, this is particularly important for slender walls, where deformation-controlled behaviour dominates.

Two principal approaches exist for evaluating the force-displacement response of structural elements. The first is the moment-curvature analysis, which integrates moment-curvature behaviour with plastic hinge analysis. The second is the direct rotation method, which relies on empirical relationships to estimate deformation capacity based on observed data. Moment-curvature analysis is a section-based approach grounded in first principles, allowing for the computation of curvature and moment capacity at various limit states. Plastic hinge analysis builds on this by converting curvature results into force-displacement relationships, using an assumed equivalent plastic hinge length to estimate total deformations. This framework has been widely used in seismic assessment and design [21,22]. In contrast, direct rotation methods, adopted in seismic guidelines such as Eurocode 8 - Part 3 [23], ASCE 41-17 [24], and ACI 369.1-22 [25], offer a more simplified approach, making them useful for practical and rapid assessments without requiring detailed sectional analysis.

While direct rotation methods offer a practical means of estimating deformation capacity, moment-curvature analysis remains a widely used analytical approach, particularly for slender walls governed by flexural behaviour. Unlike empirical methods, it establishes a direct link between displacement capacity and fundamental sectional properties, offering deeper insights into the factors influencing seismic response. Its mechanistic basis makes it adaptable to a broad range of structural configurations and construction practices, independent of regional design codes.

For slender RC walls, where flexural deformations dominate and failure is deformation-controlled, accurate estimation of displacement capacity is essential for seismic assessment and design. While moment-curvature analysis is based on well-

[1] *Associate Structural Engineer, LCI, Sydney, Arsalan.Niroomandi@lcistructures.com.au*
[2] *Ph.D. Candidate, Department of Civil and Environmental Engineering, Shiraz University of Technology, Shiraz, mahshid2774@gmail.com*
[3] *Corresponding Author, Associate Professor, Department of Civil and Environmental Engineering, Shiraz University of Technology, Shiraz, najafgholipour@sutech.ac.ir*
[4] *Professor, University of Canterbury, Christchurch, timothy.sullivan@canterbury.ac.nz (Member)*
[5] *Building Structures Director, Aurecon, Auckland, Craig.Stevenson@aurecongroup.com (Member)*

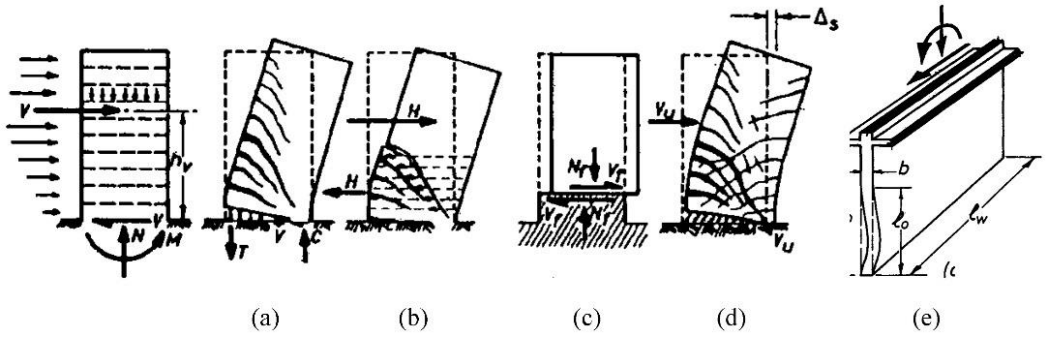

Figure 1: Failure modes in cantilever walls [26,27] ; (a) flexural yielding, (b) diagonal tension, (c) sliding shear, (d) hinge sliding and (e) lateral instability.

established structural mechanics principles, such as nonlinear material behaviour, strain compatibility, and equilibrium, plastic hinge length remains a semi-empirical parameter. It is often calibrated through equations to effectively convert plastic curvatures into global plastic displacements. Other key assumptions of the moment-curvature framework, including plane sections remaining plane, material stress-strain behaviour, and linear distribution of curvature until yield, are widely supported by foundational works such as Blume et al. [21] and Park and Paulay [22]. As these aspects are integral to the method and well-established in the literature, this study specifically focuses on the variability and limitations in existing plastic hinge length equations, recognizing their critical impact on predicting plastic displacement capacity. This refinement aims to improve the reliability of displacement estimates while maintaining consistency with the broader moment-curvature framework. Extensive research has been conducted on plastic hinge length estimation for RC walls, leading to the development of widely used empirical and semi-empirical equations. These equations were formulated based on experimental databases and theoretical considerations, each developed with specific objectives, such as optimizing plastic hinge length for certain wall configurations, failure modes, or structural conditions. While these approaches provide valuable insights, their applicability varies depending on the assumptions and datasets used in their formulation. A detailed discussion of these methods, their intended applications, and limitations is provided in the section on *Available equivalent plastic hinge length models*.

Despite these contributions, a systematic evaluation of plastic hinge length equations specifically for slender, doubly reinforced rectangular RC walls with flexural-dominated behaviour has not been conducted. Previous studies [28-32] have primarily focused on a limited range of equations or have combined databases of both squat and slender walls, without isolating those that exhibit flexural-dominated behaviour with distributed cracking.

This study aims to address these gaps by assessing the accuracy of the moment-curvature approach in estimating the displacement capacity of rectangular slender flexurally governed RC walls. This includes evaluating the performance of existing plastic hinge length equations, comparing moment-curvature-based predictions with direct rotation methods, and, if necessary, developing a more accurate plastic hinge length equation.

Slender RC walls in this study are defined as those with a shear span ratio greater than 2 [33,34], ensuring a focus on flexural behaviour. To maintain consistency with moment-curvature assumptions, specimens exhibiting single crack behaviour, or other non-flexural failure mechanisms were excluded from the database. Any wall that meets these criteria is applicable to the adopted analytical framework, regardless of its construction era, regional design standards, or specific detailing practices. Since moment-curvature analysis is grounded in first principles, its applicability is not restricted to a particular set of design provisions, provided that the selected walls exhibit flexural-dominated behaviour with distributed cracking.

To achieve these objectives, an extensive database of cyclic tests on rectangular RC slender walls with flexural failure was compiled. Displacement capacities were calculated using the moment-curvature method with various plastic hinge length equations, assessing their accuracy in predicting experimental results. These results were then compared with predictions from direct rotation methods specified in Eurocode 8 - Part 3, ASCE 41-17, and ACI 369.1-22. Based on these findings, a new plastic hinge length equation was developed to improve accuracy and reduce variability in displacement predictions, ensuring more consistent estimations for engineering applications.

FUNDAMENTALS OF THE ANALYTICAL FRAMEWORK USED

To evaluate the nonlinear behaviour of structural walls under seismic loading, it is essential to establish a robust analytical framework. The approach adopted in this study integrates moment-curvature analysis with plastic hinge analysis to estimate displacement capacity. Moment-curvature analysis provides insights into sectional behaviour, while plastic hinge analysis translates this into force-displacement relationships. This combined method enables a detailed evaluation of structural response, particularly for slender walls where flexural deformations dominate. The following sections outline the theoretical foundations, key assumptions, and material models used in this study.

Moment-Curvature and Plastic Hinge Analysis

Assumptions of Moment-Curvature Analysis

Moment-curvature analysis is based on fundamental structural mechanics principles and relies on the following key assumptions:

1. Plane sections remain plane, meaning strain distributions remain linear across the section depth.
2. A perfect bond exists between concrete and reinforcement, ensuring strain compatibility.
3. Nonlinear material behaviour is incorporated, with stress-strain relationships accounting for confinement, cyclic degradation, and strain softening effects.
4. The tensile capacity of concrete is neglected after it reaches its tensile strength, meaning that once cracking occurs, concrete is assumed to carry no further tension.

These assumptions allow for the determination of critical sectional properties, such as neutral axis depth, moment capacity, curvature at different limit states, and stiffness degradation.

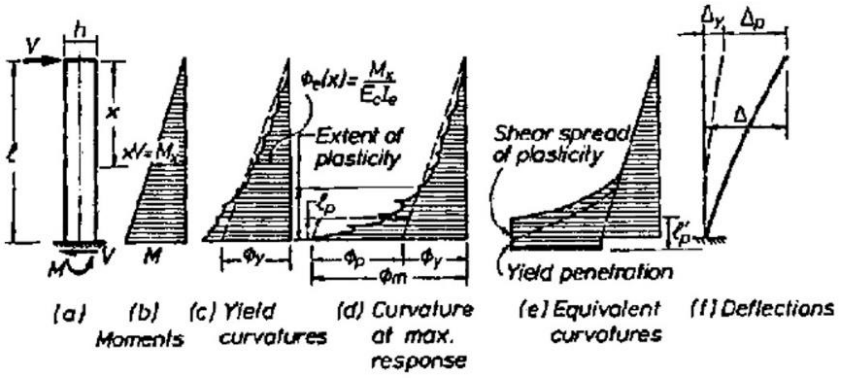

Figure 2: Moment, curvature, and deflection relationships for a reinforced concrete cantilever element subjected to a point load [27].

Plastic Hinge Analysis and Displacement Estimation

While moment-curvature analysis provides sectional response characteristics, plastic hinge analysis extends this by estimating lateral displacement. This is achieved by integrating curvature over an assumed equivalent plastic hinge length, representing the region where inelastic deformations localize after yielding (see Figure 2). Plastic hinge analysis assumes that curvature distribution is linear along the member length until yield, after which plasticity is concentrated within an equivalent plastic hinge length. This simplification allows for an effective estimation of global displacement but introduces approximations, as the actual curvature distribution beyond yield may not be perfectly localized within a single length. Despite this, the method has been widely adopted for its practicality and ability to provide reasonable estimates of displacement capacity in flexural-dominated systems.

For a cantilever wall, the displacement resulting from flexural deformations is calculated by summing the yield and plastic displacements, as outlined in Equation (1) and Equation (3). For multi storey walls, Equation (2) can be used for calculating the equivalent SDOF system yield displacement [33]. Only the flexural component is determined according to this formulation, with the shear contribution needing to be separately added if it is deemed significant.

$$\Delta'_y = \phi'_y\left(H_e + L_{sp}\right)^2/3 \qquad \phi \le \phi'_y \tag{1}$$

$$\Delta_{yi} = \frac{\varepsilon_y}{L_w} H_i^2 \left(1 - \frac{H_i}{3H_w}\right) \tag{2}$$

$$\Delta = \Delta'_y \frac{M}{M_y} + \left(\phi - \phi'_y \frac{M}{M_y}\right) L_p\left(H_e + L_{sp} - 0.5L_p\right) \qquad \phi > \phi'_y \tag{3}$$

Where, ϕ'_y is the curvature at first yield defined as the curvature at the concrete compressive strain of $\varepsilon_c = 1.8f'_c/E_c$ [35] or the yield tensile strain of the steel reinforcement, ε_y whichever occurs first, H_e is the effective height of the wall which can be assumed as $0.7H_w$ as suggested by Priestley et al. [33] for multi-storey wall buildings, $L_{sp} = 0.022f_y d_b$ is the strain penetration length into the wall foundation according to Paulay and Priestley [27]. All other parameters are defined in the notation section.

The ultimate displacement capacity of the wall is determined based on the point at which the section reaches its strain limits or key performance thresholds. In moment-curvature analysis, this occurs when either the concrete compressive strain or the tensile strain in steel reinforcement exceeds its respective capacity. The specific strain limits used in this study are detailed in the section on *Material Modelling Considerations*.

Material Modelling Considerations

Concrete Stress-Strain Model

The Mander et al. [36] model was adopted for the unconfined and confined behaviour of the concrete. The ultimate strain of concrete was defined based on Equation (4) proposed by fib [35]. This is a revised version of that originally proposed by Paulay and Priestley [27]. According to Priestley et al. [33], the concrete ultimate compression strain capacity under combined axial force and flexure is 1.3 to 1.6 times the value estimated under axial force only (e.g. Equation (4). However, such increase in the compression strain capacity of concrete when under flexure is not included in this study to align with current practice in NZ by engineers using the C5 guidelines [37].

$$\varepsilon_{cu} = \left(0.004 + \frac{0.6\rho_v f_{yh}\varepsilon_{su}}{f'_{cc}}\right) > \varepsilon_{spall} \tag{4}$$

Where, $\rho_v = \rho_{ax} + \rho_{ay}$ is the volumetric transverse reinforcement ratio and, $\rho_a = A_{sv}/(h_{core} \times s)$ is the transverse reinforcement ratio of the boundary element in x and y direction, h_{core} is the length or width of the core of the boundary element, ε_{spall} is the strain at concrete cover spalling assumed to be 0.0064 in accordance with Priestley et al. [33].

Steel Reinforcement Model

For steel reinforcement, the King et al. [38] model was adopted. The essential properties of the steel reinforcement and concrete were obtained from those reported in the tests. If data were not available, literature-recommended values were utilized. Following the guidelines from Kowalsky [39], a maximum tensile strain capacity of 6% was assumed for steel reinforcement to accommodate effects like bar buckling and cyclic degradation, even in cases where higher values were reported from uniaxial tensile tests.

Identifying Walls Applicable to the Adopted Framework

Since moment-curvature analysis relies on a flexural-dominated response, it is essential to establish clear criteria for identifying walls suitable for this framework. Walls included in this study must satisfy the following conditions:

1. Be slender, with a shear span ratio greater than 2, ensuring that flexural behaviour governs the response.
2. Have a rectangular cross-section, as non-rectangular walls (e.g., T-shaped, L-shaped, C-shaped) were not included in the experimental database.

3. Be doubly reinforced, as singly reinforced specimens were not included in the experimental database, ensuring a consistent dataset aligned with flexural design principles. These walls were excluded due to their distinct behavioural characteristics, such as single-crack formation or lateral instability, which do not align with the distributed cracking assumption of moment-curvature analysis. Additionally, singly reinforced walls are more commonly used in low-rise buildings where shear effects may dominate, making them less relevant to the study's focus on slender, flexurally governed walls.
4. Exhibit distributed cracking, meaning deformations are spread across a plastic hinge region rather than being concentrated at a single crack (see the section on *Single-Crack Walls* for further discussion).
5. Fail in a flexural-dominated mode, characterized by yielding of longitudinal reinforcement, followed by concrete crushing, bar buckling, or bar rupture, rather than shear failure or brittle failure modes (see the section on *Shear Effects in Structural Walls* for details).

Single-Crack Walls

Moment-curvature and plastic hinge analyses assume distributed cracking, meaning that deformations are spread across a region rather than being concentrated at a single crack. However, some walls exhibit single-crack behaviour, where deformations localize at a dominant crack, violating the assumptions of moment-curvature analysis.

To ensure the analytical approach aligns with observed behaviour, this study excludes single-crack walls and specimens with insufficient anchorage. Distributed cracking is assumed to occur when the probable strength of longitudinal reinforcement crossing the critical section ($A_s f_y$) is at least equal to the probable strength of longitudinal reinforcement at sections located within the plastic hinge length from the critical section. This definition is based on the *Technical Proposal to Revise the Engineering Assessment Guidelines*, Yellow Section C5 [37], where "less than half the member depth" was replaced with "plastic hinge length" to better align with the context of this study. Additionally, the flexural strength of the wall must be at least twice its cracking moment ($M_N \geq 2.0 M_{cr}$).

Shear Effects in Structural Walls

While slender walls primarily exhibit flexural behaviour, shear effects can contribute to the overall response and must be accounted for in the analysis. These effects include shear deformation, which influences total displacement, and shear strength degradation, which affects the wall's ability to resist shear forces under cyclic loading.

Shear Deformation

Shear deformation is generally small in comparison to flexural deformations in slender walls. However, it is explicitly included in this study using the method outlined in Priestley et al. [33], ensuring that its contribution to total displacement is considered. This includes both elastic and in-elastic shear deformations.

Shear Strength Degradation

Shear strength degradation occurs due to flexural cracking, which reduces shear capacity in the inelastic range. This study incorporates the shear strength degradation model by Krolicki et al. [34] to account for the interaction between flexural and shear behaviour.

ASSESSING RC SLENDER WALLS USING MOMENT-CURVATURE ANALYSIS

As outlined in the previous section and shown in Equation (3), converting the results of the moment-curvature section analysis to a force-displacement curve necessitates an equivalent plastic hinge length. A distinction is presented in Figure 2d between the equivalent plastic hinge length, denoted as L_p in Equation (3), and the distance from the column base to the level of the cross-section where no plastic strain occurs, labelled L_{pz}. This research evaluates the precision of different equivalent plastic hinge length equations by comparing the predicted ultimate displacement capacities of the walls with actual measurements (rather than the extent of strain beyond the yield point). Various formulas for calculating the equivalent plastic hinge length of RC elements are documented in the literature, some tailored specifically for RC walls. To facilitate comparison of the effectiveness of each equation, the mean ratio of the analytical to the experimental ultimate drift capacity, along with the standard deviation and coefficient of variation (COV), was computed for each formula.

Available Equivalent Plastic Hinge Length Models

This study assessed seven different equations developed to estimate the equivalent plastic flow length of RC walls. A brief description of these method is presented subsequently. All symbols are defined in the notation section.

Thomsen and Wallace (2004)

According to Thomsen and Wallace [13], the plastic hinge length of slender walls can be assumed as half of the wall length ($L_p = 0.5 L_w$). This method has been adopted in ASCE 41-17 [24].

EN1998-03 (2005)

Eurocode 8 – Part 3 [23] proposes Equation (5) for determining the plastic hinge length of RC elements (the equation has been fitted based on a database of different RC elements). In the case of Equation (5), the procedure proposed in EN1998-03 [23] is used to compute the ultimate displacement capacity of the walls which is slightly different than the approach described in the section on *Plastic Hinge Analysis* (Equation A.4 of EN1998-03, Equation (6) of this study). The main reason for this was to investigate the equation using the full procedure outlined in EN1998-03 [23].

$$L_p = \frac{H_e}{30} + 0.2 L_w + 0.11 \frac{d_b f_y}{\sqrt{f_c'}} \tag{5}$$

$$\theta_u = \frac{1}{1.7}\left(\theta_y + (\phi_u - \phi_y) L_p \left(1 - \frac{0.5 L_p}{H_e}\right)\right) \tag{6}$$

θ_y in Equation (6) can be determined using Equation (7).

$$\theta_y = \phi_y \frac{H_e + a_V z}{3} + 0.0013 + \phi_y \frac{d_b f_y}{8\sqrt{f_c'}} \tag{7}$$

Where, $a_V z$ is the tension shift of the bending moment diagram. Tension shift in RC walls is due to the spread of plasticity because of the inclined flexural-shear cracks which increases the strains in the steel reinforcement above the base [refer 33 for more information], z is the length of the internal lever arm, taken equal to $0.8 l_w$ in walls with rectangular section, $a_V = 0$ if shear cracking is not expected to precede flexural yielding at the end section; otherwise $a_V = 1$.

In Equation (7) the first term accounts for the flexural contribution, the second term represents the contribution of shear deformation and the third for anchorage slip of bars.

Priestley et al. (2007)

Priestley et al. [33] proposed Equation (8) for determining the equivalent plastic hinge length of walls.

$$L_p = kH_e + 0.1L_w + L_{sp} \tag{8}$$

$$k = 0.2\left(f_u/f_y - 1\right) \leq 0.08 \tag{9}$$

This relationship is composed of three terms including the effective height (H_e) for the flexural deformation of the wall (equivalent to the shear span of an equivalent SDOF system), the length of the wall (L_w) to account for the tension shift, and the strain penetration length into the foundation (L_{sp}), as described in the previous section.

Bohl and Adebar (2011)

Bohl and Adebar [40] developed Equation (10) for the plastic hinge length of slender walls. This relation was developed based on a numerical parametric study using nonlinear finite element software VecTor2 [41]. Equation (10) is based on the length over which the curvatures are greater than the yield (L_{pz}) and thus is not strictly the definition of plastic hinge length used traditionally (which instead is a length that gives the best relationship between the section plastic curvature and the plastic displacement).

$$L_p = (0.2L_w + 0.05H_e)\left(1 - \frac{1.5P_g}{A_g f_c'}\right) \leq 0.8L_w \tag{10}$$

Kazaz (2013)

Based on a numerical parametric study conducted using the nonlinear finite element software ANSYS, Equation (11) was developed by Kazaz [42] for determining the equivalent plastic hinge length of slender walls.

$$L_p = 0.27L_w\left(1 - \frac{P}{A_g f_c'}\right)\left(1 - \frac{f_y \rho_{sh}}{f_c'}\right)\left(\frac{H_e}{L_w}\right)^{0.45} \tag{11}$$

Where, $\rho_{sh} = A_{sh}/(s_h \times t_w)$ is the web horizontal reinforcement ratio. Kazaz [42] concluded that the equivalent plastic hinge length (L_p) of a slender wall is about half the plastic zone length (L_{pz}).

Takahashi et al. (2013)

Takahashi et al. [43] suggested that the equivalent plastic hinge length of slender walls can be determined as 2.5 times the wall thickness ($L_p = 2.5t_w$). Takahashi et al. [43] state that for the equation $L_p = 2.5t_w$ to be effective, the depth of the neutral axis must exceed the wall thickness, and the transverse reinforcement in the boundary elements should be less than half the amount stipulated by the seismic guidelines of ACI 318-08 [44]. If these conditions are not met, the equation is likely to yield an underestimation of capacity. However, they did not provide an alternative method for walls that do not satisfy these requirements.

NZ Seismic Assessment Guidelines (Yellow Section C5)

In accordance with the Technical Proposal to Revise the Engineering Assessment Guidelines, known as Yellow Section C5 [37], the ultimate rotational capacity of a slender wall (with a shear span ratio of 2 or greater) can be calculated using Equation (12). Since shear deformation is indirectly considered via β_v, therefore, further increase in the total displacement due to shear is not included when using this method. While this method has been referred to as a direct rotation method in the NZ seismic assessment guidelines, it still has the key elements of a moment-curvature analysis and therefore, it is not considered as a direct rotation method in this study.

$$\theta_u = \frac{2\beta_v \varepsilon_y H_e}{3L_w} + (K_d - 1)\phi_y L_p \tag{12}$$

Where, β_v is a dimensionless parameter that quantifies the impact of the shear span ratio on the flexural component's contribution to the overall yield deformation. For slender walls with shear span ratios between 2 to 4, β_v can be taken as the values shown in Table 1.

Table 1: β_v values for Equation (12).

$M/(VL_w)$	2	3	4	>4
β_v	1.43	1.33	1.25	1.00

The yield strain, ε_y shall not be taken greater than 0.002, $K_d = 15 - 20c/L_w$, and for plastic hinge length, L_p, the equation proposed by Priestley et al. [33] is suggested by the NZ seismic assessment guidelines (see the section on *Priestley et al. (2007)*).

Hoult (2022)

Hoult [31] proposed an empirical relation given in Equation (13) which was developed from a database of numerical and experimental results including walls with nonplanar shapes (U-shaped, T-shaped, L-shaped, H-shaped) and squat walls (e.g. shear span ratio of 1-2).

$$L_p = r(0.13L_w + 1.8H_e^{0.6})\left(1 - 0.3\frac{P}{A_g f_c'}\right) \times (1 - 0.13\,ln\,v) \tag{13}$$

$$r = \frac{\rho_{wv}}{\rho_{wv.min}} \leq 1.0 \tag{14}$$

$$\rho_{wv.min} = \frac{(t_w - n_t d_{bt}) f_{cft}}{f_u t_w} \tag{15}$$

Where, $\rho_{wv} = n_l A_s/A_g$. According to Hoult [31], the boundary element's longitudinal reinforcement ratio should be used for determining ρ_{wv} for walls with boundary elements. $f_{cft} = 0.6\sqrt{f_c'}$ is the flexural tensile strength of concrete, v = $V_{max}/\left(A_g\sqrt{f_c'}\right)$ is the shear stress parameter.

The equivalent plastic hinge length given in Equation (13) has been assessed based on the method proposed in Hoult [31] for the ultimate displacement capacity of RC walls (Equations 1-3 of Hoult [31], not given for brevity).

The primary distinction between the method applied in this study and the approach by Hoult [31] for determining the ultimate capacity of slender walls lies in the method for calculating shear deformation. In this research, the technique developed by Priestley et al. [33] was utilized, whereas Hoult [31] recommended employing the method proposed by Beyer et al. [45]. Additionally, the current study imposed a limit on the tensile strain of steel reinforcement at 6%, a constraint not required in Hoult's approach.

Selected Experimental Tests on RC Slender Walls

A database consisting of 72 slender rectangular walls subjected to in-plane cyclic loading by various researchers was compiled for this study. The main geometric and material characteristics of the test specimens are detailed in Table A1.

A significant challenge in assessing the accuracy of available plastic hinge length equations lies in choosing suitable specimens from the literature. The following criteria were applied in selecting the test specimens:

1. Specimens were tested under cyclic loading.
2. Specimens possessed a shear span ratio greater than 2.
3. Specimens had either rectangular or barbell-shaped sections.
4. Specimens were doubly reinforced with deformed longitudinal reinforcement.
5. Specimens did not have lap splices within the plastic hinge zone.
6. The behaviour of the specimens was governed by a flexural failure mode with distributed cracking.

The final 72 specimens were selected from a database of over 300 walls, ensuring that only those meeting the defined flexural-dominated behaviour criteria were included.

The selected walls exhibited flexurally governed behaviour, with observed failure modes including concrete crushing, bar buckling, and bar rupture. Some walls also exhibited lateral instability; however, these specimens demonstrated significant flexural behaviour prior to instability, making them relevant to this study. It is noted that most original experimental reports did not explicitly classify whether failure was dominated by concrete crushing, bar buckling, or bar rupture, as these mechanisms often co-occur in flexural failures. Given this limitation, the selection process prioritized ensuring flexural-dominated behaviour with distributed cracking, rather than attempting to categorize the primary flexural failure mechanism for each individual specimen.

For specimens R1, W4, and SW2-1, significant differences were observed between analytical and experimental results regarding yield drift and initial stiffness. Given that this study primarily aims to estimate plastic drift, the analytical yield drift values for these walls were adjusted to align with experimental findings.

Evaluation of the Equivalent Plastic Hinge Length Models against Experimental Results

To evaluate the accuracy of equations for estimating the equivalent plastic hinge length in slender walls, force-displacement curves and ultimate drift capacities were determined using the relations described in the section on *Available equivalent plastic hinge length models* and compared with experimental results. The ultimate displacement capacity was defined as the displacement at the top of the wall corresponding to a 20% reduction in lateral strength, a criterion widely adopted in earthquake engineering literature (e.g., Paulay and Priestley 1992) and seismic assessment standards such as ASCE 41 and the New Zealand seismic assessment guidelines. Therefore, this strength degradation threshold is considered to corresponds to the life safety limit state, where significant material degradation (e.g., concrete crushing, bar buckling) occurs, but the structure is still expected to maintain residual capacity. While this 20% strength reduction is a well-established benchmark, it is somewhat arbitrary, as different values (e.g., 15% or 25%) could be considered in other contexts. The choice of a 20% drop, as opposed to another percentage, could influence the evaluation of prediction methods, highlighting an area for potential refinement in future research.

For the moment-curvature behaviour of rectangular walls, a section analysis was performed using CUMBIA [46], except for the walls with barbell-shaped sections, where SAP2000 [47] was utilized (specimens B1, B3, B10, WB, and W-1).

Analytical vs Experimental Results

Figure 3 displays the force-displacement curves for chosen specimens, comparing the experimental outcomes with the analytical results obtained from the different equivalent plastic hinge length equations.

Figure 4 displays the predicted drift capacity of the specimens, calculated using various equivalent plastic hinge length equations, and compares these predictions to the experimental drift capacities. The plotted curves highlight the variability in each prediction method. To facilitate a more detailed comparison, Table 2 includes the mean, standard deviation, and coefficient of variation for the ratios of the estimated to the experimental drift capacities for each method. A mean value above one indicates that the equation tends to overestimate the drift capacity of the wall. Assessing the effectiveness of plastic hinge length models requires consideration of both the average results and their variability.

Discussion of the Results

Based on the results presented in Table 2, the following observations can be made:

1. For seismic evaluations where accurate drift capacity is crucial, the equation proposed by Bohl and Adebar [40] offered the most reliable indication of the average capacity.
2. The equations proposed by Priestley et al. [33], Kazaz [42] and Hoult [31] overestimate the mean displacement capacity.
3. The method proposed by Takahashi et al. [43] and NZ Yellow Section C5 [37] underestimate the results. The method presented by Takahashi et al. was not clear regarding whether the thickness in their equation referred to the wall thickness or the thickness of boundary elements. Consequently, both interpretations were explored. It was found that using the thickness of the walls yield better COV. Therefore, the results shown in Table 2 are for the thickness of the wall and not the boundary elements. If the standard deviation (or COV) of the results is key, then Takahashi et al. [43] method can be considered best.
4. The method proposed by EN1998-03 [23] considerably underestimates the displacement capacity of slender walls. However, it was found that this is mainly due to the inherent conservatism in Equation A.4 of EN1998-03 (Equation (6)), and not necessarily the plastic hinge length equation itself.
5. The equation proposed by Thomsen and Wallace [13] considerably overestimates the displacement capacity. Therefore, it is not suitable for assessment or design purposes.

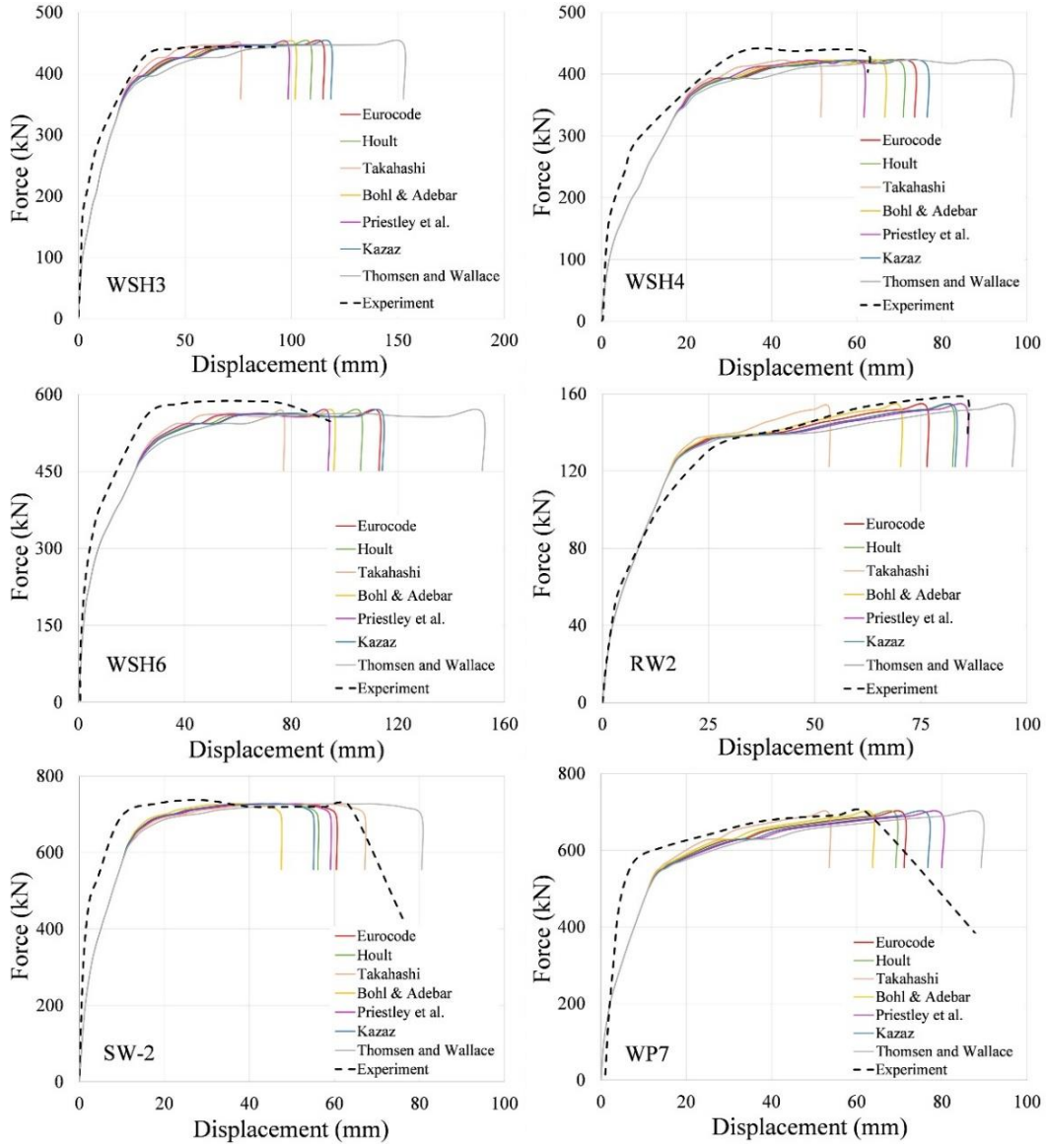

Figure 3: Force-displacement curves of selected specimens – Analytical vs Experiential results.

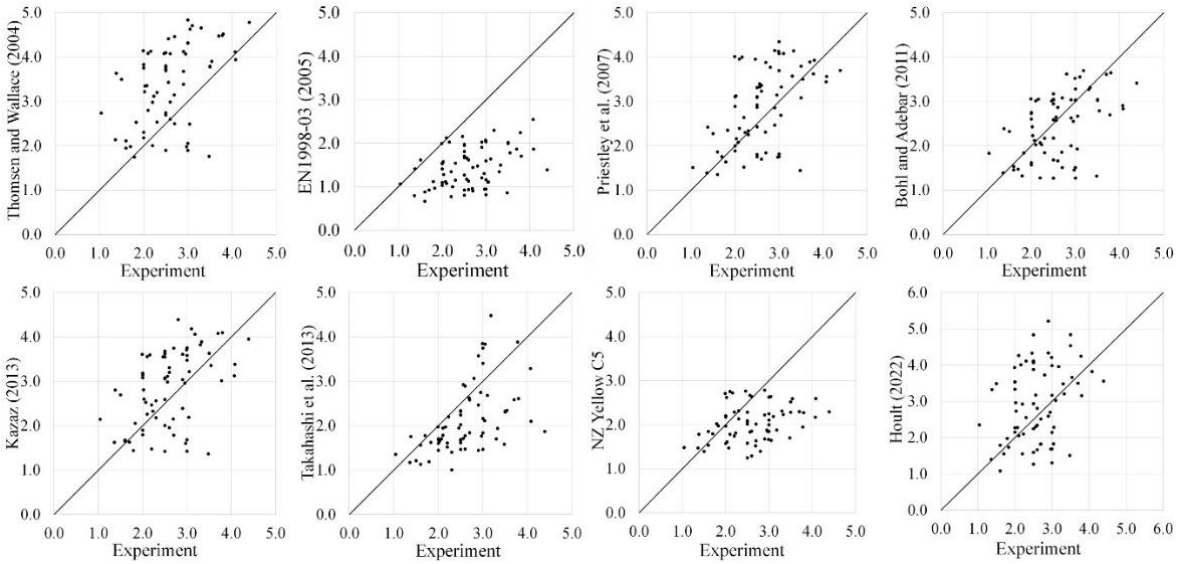

Figure 4: Comparison of the analytical vs. experimental drift capacities of the test specimens.

Table 2: Evaluation of the analytical drift vs experimental results.

Method	Analytical/Experimental Drift Ratio		
	Mean	Standard Deviation	COV
Thomsen and Wallace [13]	1.39	0.43	0.31
EN1998-3 [23]	0.57	0.20	0.34
Priestley et al. [33]	1.14	0.33	0.29
Bohl and Adebar [40]	0.98	0.29	0.30
Kazaz [42]	1.14	0.35	0.31
Takahashi et al. [43]	0.82	0.23	0.28
NZ Yellow Section C5 [37]	0.83	0.24	0.29
Hoult [31]	1.19	0.47	0.39

PROPOSED PLASTIC HINGE LENGTH EQUATION

As discussed in the previous section, none of the existing equations in the literature simultaneously achieve high accuracy and low variability. While some equations provide accurate mean predictions, they often exhibit high variability, whereas others offer lower variability but compromise accuracy. Consequently, there is a need for a more refined equation that balances both aspects.

This study identified that Bohl's equation provides one of the most accurate mean predictions, while Takahashi's equation demonstrates lower variability. The proposed Equation (16) combines these advantages by maintaining the accuracy of Bohl's mean prediction while reducing the coefficient of variation (COV) by 15%, improving the consistency of plastic hinge length estimations. This formulation results in a mean of 0.99 and a COV of 0.26, providing a more reliable and practical equation for engineers assessing plastic hinge length in slender RC walls.

$$L_p = 0.02H_e + 0.12L_w + 1.4t_w \tag{16}$$

It was possible to develop an equation including strain penetration length in the format of $ad_b f_y/\sqrt{f_c'}$. However, it had minimal impact on COV, and would further complicate the equation. It is worth noting that since parameters such as axial load, transverse reinforcement, and neutral axis depth are already accounted for in the moment-curvature analysis, they have little effects on the ideal equation for the plastic hinge length itself.

ASSESSING RC SLENDER WALLS USING DIRECT ROTATION METHOD

An alternative to the moment-curvature analysis is the direct rotation method. This section evaluates the accuracy of the approaches recommended in EN1998-3 [23], ASCE 41-17 [24], and ACI 369.1-22 [25] for determining the drift capacity of slender RC walls.

EN1998-3 (2005)

EN1998-3 [23] incorporates Equation (17) for determining the ultimate total rotation capacity, θ_u, of reinforced concrete walls under cyclic loading. This is an empirical equation developed for different types of RC elements with modifications for RC walls.

$$\theta_u = \theta_y + \frac{0.6}{1.8}0.0145 \times 0.25^{\upsilon}\left[\frac{max(0.01;\omega')}{max(0.01;\omega)}\right]^{0.3} \times f_c'^{0.2}\left(min\left(9;\frac{H_e}{l_w}\right)\right)^{0.35} \times 25^{\left(\alpha\rho_{ax}\frac{f_{yh}}{f_c'}\right)} \times (1,275^{100\rho_d}) \tag{17}$$

Where, θ_y can be determined using Equation (7). $\upsilon = P/(A_g f_c')$, P is the axial force (positive for compression), ω, ω' are the mechanical reinforcement ratio of the tension and compression longitudinal reinforcement (including the web reinforcement), respectively, ρ_d is the steel ratio of diagonal reinforcement (if any), in each diagonal direction, α is the confinement effectiveness factor and can be determined using Equation (18).

$$\alpha = \left(1 - \frac{s}{2b_0}\right)\left(1 - \frac{s}{2h_0}\right)\left(1 - \frac{\sum b_i^2}{6h_0 b_0}\right) \tag{18}$$

Where, b_0 and h_0 are the dimension of confined core to the centreline of the hoop, b_i is the centreline spacing of longitudinal bars (indexed by i) laterally restrained by a stirrup corner or a cross-tie along the perimeter of the cross-section.

ASCE 41-17

The plastic rotation capacity of structural walls, which are primarily flexure-governed, can be calculated using Table 10-9 from ASCE 41-17 [24]. Walls with boundary elements that have a transverse reinforcement spacing exceeding $8d_b$ are classified as unconfined. For boundary elements deemed confined, ASCE 41-17 [24] references the specifications of ACI 318 [48]. However, it remains uncertain which specific provisions of ACI 318, including ductility levels, are applicable. In this analysis, any boundary elements with a transverse reinforcement spacing less than $8d_b$ are considered confined. The plastic rotation capacities derived from Table 10-9 of ASCE 41-17 have yielded conservative figures (refer to Figure 5) and are thus regarded as the upper limits for applying the ASCE 41-17 methodology. Walls that do not comply with the ACI 318 requirements will have lower average plastic rotation capacities under the ASCE 41-17 criteria. It is worth noting that the plastic rotation capacities obtained from ASCE 41-17 provisions are determined based on 20% reduction of strength to represent concrete crushing and bar buckling for flexural members. To determine the yield drift of slender walls, ASCE 41-17 suggest using Equation (19).

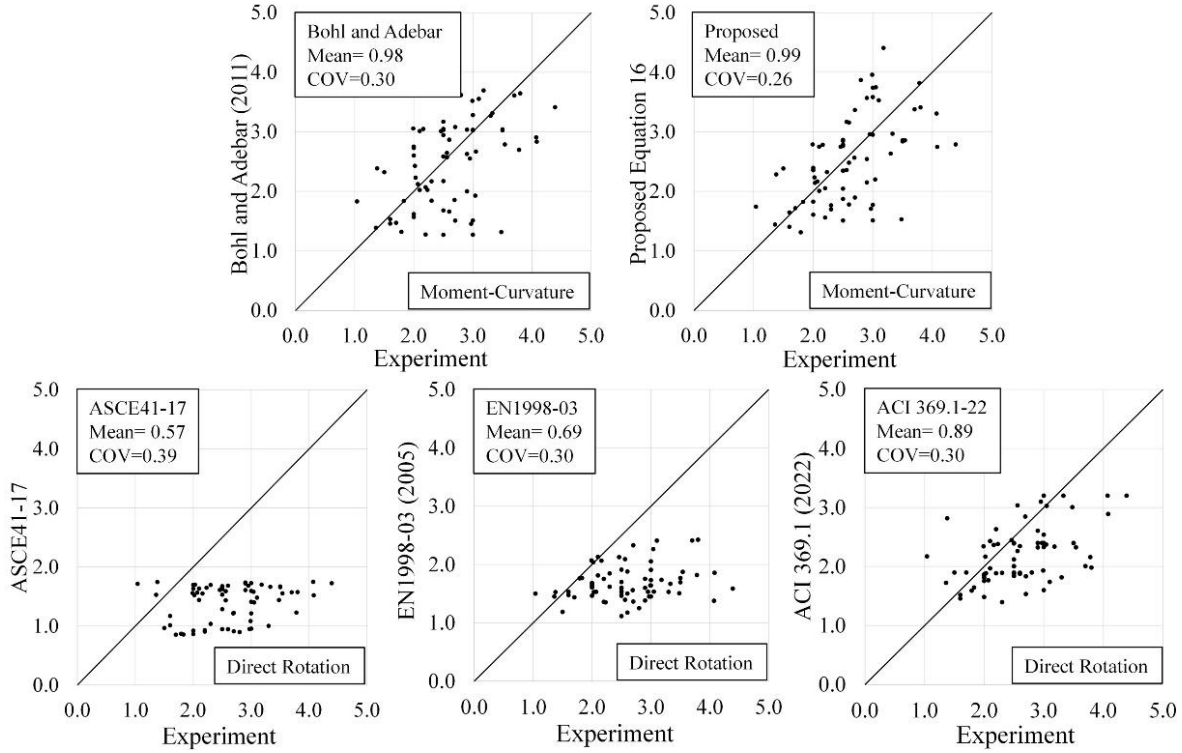

Figure 5: Moment-curvature vs direction rotation methods.

$$\theta_y = \left(\frac{M_y}{(EI)_{eff}}\right) L_p = \phi_y L_p \tag{19}$$

Where, $L_p = 0.5L_w$, and ϕ_y can be determined using a moment-curvature analysis.

ACI 369.1-22

One of the most recent methods based on a direct rotation approach for determining the rotation capacity of RC structural walls controlled by flexure is the one proposed in ACI 369.1-22 [25], Table 7.4.1.1.a and 7.4.1.1.b. This method has been also referred to in ASCE 41-23. An interesting aspect of this method is that instead of determining the plastic rotation capacity, the total rotation capacity of the walls can be directly calculated. This is different than the previous methods in which the yield and plastic rotation capacities should be determined separately. In this study, $w_v V_{MCultDE} = V_{max}$ was used.

Where, V_{max} is the maximum base shear of the wall from the experiments.

Discussion of the Results

Figure 5 compares the analytical vs experimental rotation capacities utilising alternative direct rotation methods and moment-curvature analysis (based on the Bohl and Adebar [40] equation and Equation (16) proposed in this study). The moment-curvature method demonstrates a more accurate alignment with the test data in terms of Mean and COV when compared to the direct rotation methods, when using the proposed method.

It was found that the accuracy of direct rotation methods decreases with thicker walls (over 200 mm). When the walls have a smaller section aspect ratio (L_w/t_w), particularly in accordance with ASCE41-17 and EN1998-03 standards, the accuracy of the results also declined. The direct rotation method proposed in ACI 369.1-22 [25] achieved a better accuracy compared to those proposed in ASCE 41-17 and EN1998-3.

SUMMARY AND CONCLUSIONS

The seismic assessment and design of slender RC walls require accurate prediction of displacement capacity, particularly for walls governed by flexural behavior and deformation-controlled failure modes. Moment-curvature analysis, when paired with an appropriate plastic hinge length equation, provides a mechanistic framework for estimating deformation capacity, linking sectional curvatures to global displacements based on first principles. However, the accuracy of plastic hinge length equations, which are often semi-empirical, varies significantly, affecting the reliability of displacement predictions.

This study systematically evaluated seven existing plastic hinge length equations using a database of 72 slender RC wall specimens subjected to cyclic loading. The research aimed to assess their accuracy, identify limitations, and, if necessary, propose an improved formulation to enhance prediction consistency and reliability. Additionally, the study compared moment-curvature-based predictions with direct rotation methods, which provide an alternative approach for estimating deformation capacity.

Key findings include:

1. Among the existing models, Bohl and Adebar's (2011) equation provided the closest match to the mean experimental drift capacity but exhibited high variability, with a CoV of 0.30. Other equations also showed inconsistencies, particularly in their ability to accurately predict ultimate drift capacities.
2. A new plastic hinge length equation was developed, achieving a mean analytical-to-experimental drift capacity ratio of 0.99 and a CoV of 0.26, the lowest among the evaluated equations. The proposed equation enhances prediction accuracy while being simple and user-friendly, making it more accessible for engineering applications.
3. For slender, flexurally governed RC walls, moment-curvature analysis using an appropriate plastic hinge length equation outperformed direct rotation methods, including

those in EN1998-03, ASCE 41-17, and ACI 369.1-22. Direct rotation methods exhibited higher CoV values (~0.30) and generally conservative estimates of ultimate drift capacity, reinforcing the suitability of moment-curvature-based approaches for assessing slender walls.

These findings reaffirm the robustness of moment-curvature analysis for the seismic assessment of slender RC walls and highlight the importance of selecting an appropriate plastic hinge length equation to improve prediction reliability. The proposed equation provides a refined, practical alternative to existing models, enabling more accurate and consistent displacement capacity estimates, which are critical for seismic design and assessment.

PRACTICAL TOOL FOR ENGINEERS: CUMBIA-WALLS

To facilitate the practical application of the findings from this study, the analytical framework, including moment-curvature and plastic hinge length analysis, is implemented in the CUMBIA-WALLS software. This tool is freely available on GitHub for engineers and researchers interested in conducting seismic performance evaluations of RC walls.

We encourage engineers to explore and utilize CUMBIA-WALLS for enhanced accuracy and efficiency in their seismic design and evaluation processes. Feedback and contributions from the engineering community are welcome to further improve this open-source platform. CUMBIA-WALLS can be found from: https://github.com/LuisMontejo/CUMBIA-Walls.

LIMITATIONS

The proposed method is validated for slender, doubly reinforced rectangular RC walls with a shear span ratio greater than 2, governed by flexural behaviour with distributed cracking. It is not applicable to singly reinforced walls, non-rectangular wall cross-sections (e.g., T-shaped, L-shaped, or barbell walls), shear-dominated walls, or those exhibiting single-crack mechanisms, as these behaviours were not represented in the experimental database. While shear deformations and shear strength degradation are considered, the method's accuracy in predicting shear- or shear-flexure-governed failures has not been assessed. These limitations should be considered when applying the proposed approach beyond its validated scope.

Data Availability Statement

The data supporting the findings of this study are available upon reasonable request from the corresponding author.

NOTATIONS

A_g = Gross area of the wall's section,

A_s = Area of a single longitudinal bar,

A_{sh} = Web horizontal reinforcement area,

A_{sv} = Transverse reinforcement area,

H_e = Effective height of the wall,

H_w = Total height of the wall,

L_p = Equivalent plastic hinge length,

L_{pz} = Distance from the column base to the cross-sectional level with zero plastic strain,

L_{sp} = Strain penetration length,

L_w = Length of the wall,

M_y = Moment capacity at first yield,

P = Axial load on the wall,

P_g = Axial load on the wall due to gravity,

V_{max} = Maximum base shear of the wall,

c = Neutral axis depth,

d_b = Diameter of the tension bars,

d_{bt} = Diameter of the transverse shear reinforcement,

f_{cft} = Flexural tensile strength of concrete,

f_y = Yield stress of longitudinal bars,

f_{yh} = Yield stress of the transverse reinforcement,

f_u = Ultimate stress of longitudinal bars,

f_c' = Concrete compressive strength,

f_{cc}' = Concrete compressive strength of the confined section,

h_{core} = Length or width of the core of the boundary element,

n_l = Number of longitudinal bars,

n_t = Number of transverse bar layers,

s = Transverse reinforcement spacing,

s_h = Web horizontal reinforcement spacing

t_w = Thickness of the wall,

z = Length of the internal lever arm,

α = Confinement effectiveness factor,

$a_V z$ = Tension shift of the bending moment diagram,

ε_y = Yield strain of longitudinal bars,

ε_{spall} = Strain at concrete cover spalling,

ε_{su} = Ultimate strain of the transverse reinforcement,

υ = Shear stress parameter,

ρ_a = Transverse reinforcement ratio of the boundary element in x and y direction,

ρ_{sh} = Web horizontal reinforcement ratio,

ρ_v = Volumetric transverse reinforcement ratio,

ρ_{wv} = Longitudinal reinforcement ratio,

ϕ_y' = Curvature at first yield,

ϕ_y = Curvature at yield,

θ_y = Yield rotation capacity of the wall,

θ_u = Ultimate total rotation capacity of the wall,

Δ_y' = Displacement at first yield,

REFERENCES

1 Paulay T, Priestley M and Synge A (1982). "Ductility in earthquake resisting squat shearwalls". *ACI Journal Proceedings*, **79**(4): 257-269. https://doi.org/10.14359/10903

2 Maffei J, Bonelli P, Kelly D, Lehman DE, Lowes L, Moehle J, Telleen K, Wallace J and Willford M (2014). "*Recommendations for Seismic Design of Reinforced Concrete Wall Buildings Based on Studies of the 2010 Maule, Chile Earthquake*". NIST GCR 14-917-25, National Institute of Standards and Technology, Gaithersburg, MD, 322pp.

3 Kam WY, Pampanin S and Elwood K (2011). "Seismic performance of reinforced concrete buildings in the 22 February Christchurch (Lyttleton) earthquake". *Bulletin of the New Zealand Society for Earthquake Engineering*, **44**(4): 239-278. https://doi.org/10.5459/bnzsee.44.4.239-278

4 Sritharan S, Beyer K, Henry RS, Chai Y, Kowalsky M and Bull D (2014). "Understanding poor seismic performance of concrete walls and design implications". *Earthquake Spectra*, **30**(1): 307-334. https://doi.org/10.1193/021713EQS036M

5 Wood SL (1991). "Performance of reinforced concrete buildings during the 1985 Chile earthquake: implications for the design of structural walls". *Earthquake Spectra*, **7**(4): 607-638. https://doi.org/10.1193/1.1585645

6 Connor IN (1985). "The san antonio, Chile, earthquake of 3 March 1985". *Bulletin of the New Zealand Society for Earthquake Engineering*, **18**(2): 128-138. https://doi.org/10.5459/bnzsee.18.2.128-138

7 Muguruma H, Nishiyama M and Watanabe F (1995). "Lessons learned from the Kobe earthquake—A Japanese perspective". *Pci Journal*, **40**(4): 28-42. https://doi.org/10.15554/pcij.07011995.28.42

8 Dazio A, Beyer K and Bachmann H (2009). "Quasi-static cyclic tests and plastic hinge analysis of RC structural walls". *Engineering Structures*, **31**(7): 1556-1571. https://doi.org/10.1016/j.engstruct.2009.02.018

9 Oesterle R, Fiorato A, Johal L, Carpenter J, Russell H and Corley W (1976)."*Earthquake Resistant Structural Walls-Tests of Isolated Walls*". NSF/RA-760815, Research and Development Construction Technology Laboratories, Portland Cement Association, Washington, D.C, 328pp.

10 Segura Jr CL and Wallace JW (2018). "Seismic performance limitations and detailing of slender reinforced concrete walls". *ACI Structural Journal*, **115**(3): 849-859. https://doi.org/10.14359/51701918

11 Shegay A, Dashti F, Hogan L, Lu Y, Niroomandi A, Seifi P, Zhang T, Dhakal R, Elwood K and Henry R (2020). "Research programme on seismic performance of reinforced concrete walls: Key recommendations". *Bulletin of the New Zealand Society for Earthquake Engineering*, **53**(2): 54-69. https://doi.org/10.5459/bnzsee.53.2.54-69

12 Niroomandi A, Pampanin S, Dhakal RP, Ashtiani MS and Nokes R (2021). "Experimental study on the effects of bi-directional loading pattern on rectangular reinforced concrete walls". *Earthquake Engineering and Structural Dynamics*, **50**(7): 2010-2030. https://doi.org/10.1002/eqe.3433

13 Thomsen IV JH and Wallace JW (2004). "Displacement-based design of slender reinforced concrete structural walls—experimental verification". *Journal of Structural Engineering*, **130**(4): 618-630. https://doi.org/10.1061/(ASCE)0733-9445(2004)130:4(618)

14 Dashti F, Dhakal RP and Pampanin S (2017). "Tests on slender ductile structural walls designed according to New Zealand Standard". *Bulletin of the New Zealand Society for Earthquake Engineering*, **50**(4): 504-516. https://doi.org/10.5459/bnzsee.50.4.504-516

15 Paulay T and Goodsir WJ (1985). "The ductility of structural walls". *Bulletin of the New Zealand Society for Earthquake Engineering*, **18**(3): 250-269. https://doi.org/10.5459/bnzsee.18.3.250-269

16 Tripathi M, Dhakal RP and Dashti F (2019). "Bar buckling in ductile RC walls with different boundary zone detailing: Experimental investigation". *Engineering Structures*, **198**: 109544. https://doi.org/10.1016/j.engstruct.2019.109544

17 Oesterle R, Aristizabal-Ochoa J, Fiorato A, Russell H and Corley W (1979)."*Earthquake resistant structural walls-tests of isolated walls-phase II*". NSF/RA-790275, Construction Technology Laboratories, Portland Cement Association, Washington, D.C, 345pp.

18 Lu Y, Gultom RJ, Ma QQ and Henry RS (2018). "Experimental Validation of Minimum Vertical Reinforcement Requirements for Ductile Concrete Walls". *ACI Structural Journal*, **115**(4): 1115-1130. https://doi.org/10.14359/51702048

19 Niroomandi A, Pampanin S, Dhakal RP and Soleymani Ashtiani M (2022). "Seismic behavior of rectangular reinforced concrete walls prone to out-of-plane shear-axial failure under bidirectional loading". *Journal of Structural Engineering*, **148**(10): 04022166. https://doi.org/10.1061/(asce)st.1943-541x.0003467

20 Niroomandi A, Pampanin S, Dhakal RP, Ashtiani MS and Torre Cdl (2022). "Out-of-plane shear-axial failure in slender rectangular reinforced concrete walls". *Earthquake Engineering and Structural Dynamics*, **51**(10): 2426-2448. https://doi.org/10.1002/eqe.3670

21 Blume JA, Newmark NM and Corning LH (1961). *Design of Multistory Reinforced Concrete Buildings for Earthquake Motions*. Portland Cement Association Chicago, United States, 318pp.

22 Park R and Paulay T (1975). *Reinforced Concrete Structures*. ISBN 978-0-471-65917-4, John Wiley & Sons, Egypt, 769pp.

23 EN1998-3 (2005)."*Eurocode 8: Design of Structures for Earthquake Resistance—Part 3: Assessment and Retrofitting of Buildings*". European Committee for Standardization (CEN), Brussels, Belgium, 89pp.

24 ASCE41-17 (2017)."*Seismic Evaluation and Retrofit of Existing Buildings*". American Society of Civil Engineers (ASCE), Reston, Virginia, USA, 576pp.

25 ACI369.1-22 (2022)."*Seismic Evaluation and Retrofit of Existing Concrete Buildings*". American Concrete Institute (ACI), Farmington Hills, Michigan, USA, 125pp.

26 Paulay T and Priestley MJN (1993). "Stability of ductile structural walls". *ACI Structural Journal*, **90**(4): 385-392.

27 Paulay T and Priestley MN (1992). *Seismic Design of Reinforced Concrete and Masonry Buildings*. ISBN 978-0-471-54915-4, John Wiley & Sons, Inc., New York, USA.

28 Cordero M, Fox MJ and Sullivan TJ (2015). "Assessing simplified expressions for the deformation capacity of RC walls". *Tenth Pacific Conference on Earthquake Engineering*, November 6-8, Sydney, Australia, 8pp.

29 Puranam A, Wang Y and Pujol S (2018). "Estimating Drift Capacity of Reinforced Concrete Structural Walls". *ACI Structural Journal*, **115**(6): 1563-1575. https://doi.org/10.14359/51702444

30 Hoult R, Goldsworthy H and Lumantarna E (2018). "Plastic hinge length for lightly reinforced rectangular concrete walls". *Journal of Earthquake Engineering*, **22**(8): 1447-1478. https://doi.org/10.1080/13632469.2017.1286619

31 Hoult R (2022). "Universal plastic hinge length for reinforced concrete walls". *ACI Structural Journal*, **119**(4): 75-83. https://doi.org/10.14359/51734650

32 Niroomandi A, Stevenson C, Najafgholipour MA, Firoozbakhtian M and Sullivan T (2023). "Seismic Behaviour of Slender Rectangular Reinforced Concrete Walls based on analytical methods". *The New Zealand Society for Earthquake Engineering (NZSEE) Annual Technical Conference*, Auckland, New Zealand, 16pp.

33 Priestley MJN, Calvi GM and Kowalsky MJ (2007). *Displacement-Based Seismic Design of Structures*. ISBN 978-88-6198-000-6, IUSS Press, Pavia, Italy, 721pp.

34 Krolicki J, Maffei J and Calvi GM (2011). "Shear strength of reinforced concrete walls subjected to cyclic loading". *Journal of Earthquake Engineering*, **15**(S1): 30-71. https://doi.org/10.1080/13632469.2011.562049

35 FIB25 (2003). "Displacement-based seismic design of reinforced concrete buildings". *Federación Internacional para Concreto Estructural*.

36 Mander JB, Priestley MJ and Park R (1988). "Theoretical stress-strain model for confined concrete". *Journal of Structural Engineering*, **114**(8): 1804-1826.

37 MBIE (2018)."*The NZ Seismic Assessment of Existing Buildings: Draft Revision to Section C5 Concrete Buildings*". Ministry of Business, Innovation and Employment (MBIE), Wellington, NZ.

38 King DJ, Priestley MJN and Park R (1986). *Computer Programs for Concrete Column Design*. University of Canterbury.

39 Kowalsky MJ (2000). "Deformation limit states for circular reinforced concrete bridge columns". *Journal of Structural Engineering*, **126**(8): 869-878.

40 Bohl A and Adebar P (2011). "Plastic hinge lengths in high-rise concrete shear walls". *ACI Structural Journal*, **108**(2): 148.

41 Wong P and Vecchio F (2002). *VecTor2 and FormWorks User's Manual (Publication No. 2002-02)*. Toronto, ON, Canada: University of Toronto, Department of Civil Engineering.

42 Kazaz İ (2013). "Analytical study on plastic hinge length of structural walls". *Journal of Structural Engineering*, **139**(11): 1938-1950. https://doi.org/10.1061/(ASCE)ST.1943-541X.0000770

43 Takahashi S, Yoshida K, Ichinose T, Sanada Y, Matsumoto K, Fukuyama H and Suwada H (2013). "Flexural drift capacity of reinforced concrete wall with limited confinement". *ACI Structural Journal*, **110**(1): 95-104. https://doi.org/10.14359/51684333

44 ACI318-08 (2008)."*Building Code Requirements for Structural Concrete and Commentary*". American Concrete Institute (ACI), Farmington Hills, USA, 456pp.

45 Beyer K, Dazio A and Priestley N (2011). "Shear deformations of slender reinforced concrete walls under seismic loading". *ACI Structural Journal*, **108**(2): 167-177. https://doi.org/10.14359/51664252

46 Montejo L and Niroomandi A (2021). *Cumbia-Walls-set of codes for the analysis of reinforced concrete walls*.

47 SAP2000 Version 21.0.2 (2019). *Integrated Finite Element Analysis and Design of Structures*. Computers and Structures Inc, Berkeley, California, USA.

48 ACI318-19 (2019)."*Building Code Requirements for Structural Concrete and Commentary*". American Concrete Institute (ACI), Farmington Hills, USA, 624pp.

49 Pilakoutas K and Elnashai A (1995). "Cyclic behavior of RC cantilever walls, part I: Experimental results". *ACI Structural Journal*, **92**(3): 271-281. https://doi.org/10.14359/1128

50 Thomsen JH and Wallace JW (1995). *Displacement-Based Design of RC Structural Walls: an Experimental Investigation of Walls with Rectangular and T-shaped Cross-Sections*. Clarkson University, Department of Civil Engineering, New York, USA, 706pp.

51 Tupper B (1999). "*Seismic Response of Reinforced Concrete Walls with Steel Boundary Elements*". Master Thesis, McGill University.

52 Oh YH, Han SW and Lee LH (2002). "Effect of boundary element details on the seismic deformation capacity of structural walls". *Earthquake Engineering and Structural Dynamics*, **31**(8): 1583-1602. https://doi.org/10.1002/eqe.177

53 Mobeen SS (2002). "*Cyclic Tests of Shear Walls Confined with Double Head Studs*". Master Thesis, University of Alberta.

54 Han S, Oh Y-H and Lee L-H (2002). "Seismic behaviour of structural walls with specific details". *Magazine of Concrete Research*, **54**(5): 333-345. https://doi.org/10.1680/macr.2002.54.5.333

55 Liu H (2004). "*Effect of Concrete Strength on the Response of Ductile Shear Walls*". Master Thesis, McGill University Montreal, Canada.

56 Ghorbani-Renani I, Velev N, Tremblay R, Palermo D, Massicotte B and Léger P (2009). "Modeling and testing influence of scaling effects on inelastic response of shear walls". *ACI Structural Journal*, **106**(3): 358-367. https://doi.org/10.14359/56500

57 Tran TA (2012). "*Experimental and Analytical Studies of Moderate Aspect ratio Reinforced oncrete Structural Walls*". PhD Dissertation, University of California, Los Angeles (UCLA).

58 Christidis K, Vougioukas E and Trezos KG (2013). "Seismic assessment of existing RC shear walls non-compliant with current code provisions". *Magazine of Concrete Research*, **65**(17): 1059-1072. https://doi.org/10.1680/macr.13.00051

59 Villalobos E (2014). "*Response of Reinforced Concrete Structural Walls with Discontinuities in their Geometry and Reinforcement Configuration*". PhD Dissertation, Purdue University.

60 Hube M, Marihuén A, de la Llera JC and Stojadinovic B (2014). "Seismic behavior of slender reinforced concrete walls". *Engineering Structures*, **80**: 377-388. https://doi.org/10.1016/j.engstruct.2014.09.014

61 Christidis KI, Vougioukas E and Trezos KG (2016). "Strengthening of non-conforming RC shear walls using different steel configurations". *Engineering Structures*, **124**: 258-268. https://doi.org/10.1016/j.engstruct.2016.05.049

62 Lu Y, Henry RS, Gultom R and Ma QT (2017). "Cyclic testing of reinforced concrete walls with distributed minimum vertical reinforcement". *Journal of Structural Engineering*, **143**(5): 04016225. https://doi.org/10.1061/(ASCE)ST.1943-541X.0001723

63 Zhu Z and Guo Z (2017). "Experimental study on emulative hybrid precast concrete shear walls". *KSCE Journal of Civil Engineering*, **21**(1): 329-338. https://doi.org/10.1007/s12205-016-0620-4

64 Abdulridha A and Palermo D (2017). "Behaviour and modelling of hybrid SMA-steel reinforced concrete slender shear wall". *Engineering Structures*, **147**: 77-89. https://doi.org/10.1016/j.engstruct.2017.04.058

65 Zhi Q, Guo Z, Xiao Q, Yuan F and Song J (2017). "Quasi-static test and strut-and-tie modeling of precast concrete shear walls with grouted lap-spliced connections". *Construction and Building Materials*, **150**: 190-203. https://doi.org/10.1016/j.conbuildmat.2017.05.183

66 Shegay A, Motter C, Henry R and Elwood K (2017). "Experimental study on reinforced concrete walls with high axial loads". *2017 NZSEE Annual Conference*, Wellington, New Zealand, 8pp.

67 Yuan W, Zhao J, Sun Y and Zeng L (2018). "Experimental study on seismic behavior of concrete walls reinforced by PC strands". *Engineering Structures*, **175**: 577-590. https://doi.org/10.1016/j.engstruct.2018.08.091

68 Zhu Z and Guo Z (2019). "Seismic behavior of precast concrete shear walls with different confined boundary elements". *KSCE Journal of Civil Engineering*, **23**(2): 711-718. https://doi.org/10.1007/s12205-018-0700-8

APPENDIX

Table A1: Database of the RC walls used for the study.

Reference	Wall ID	$\frac{M}{VL_w}$	$\frac{P}{A_g f_c^{'}}$	H_e mm	L_w mm	t_w mm	d_b mm	ρ_v	$\frac{\delta_u}{H_{eff}}$ %
Oesterle et al. [9]	R1	2.4	0	4572	1905	102	9.5	0.008	2.3
	R2	2.4	0	4572	1905	102	12.7	0.021	2.9
	B1	2.4	0	4572	1905	305	12.7	0.002	3.3
	B3	2.4	0	4572	1905	305	12.7	0.021	4.39
Oesterle et al. [17]	B10	2.4	0.08	4572	1905	305	15.9	0.020	3.33
Pilakoutas & Elnashai [49]	SW4	2	0	1200	600	60	12	0.009	1.79
	SW6	2	0	1200	600	60	12	0.005	1.83
	SW8	2	0	1200	600	60	10	0.004	2
	SW9	2	0	1200	600	60	10	0.005	2.1
Thomsen & Wallace [50]	RW1	3.13	0.1	3810	1219	102	9.5	0.012	2.2
	RW2	3.13	0.07	3810	1219	102	9.5	0.013	2.3
Tupper [51]	W3	3.75	0.11	3750	1000	152	19.5	0.010	3.04
Oh et al. [52]	WR20	2	0.1	3000	1500	200	12.7	0.012	2.7
	WR10	2	0.1	3000	1500	200	12.7	0.023	2.9
	WR0	2	0.1	3000	1500	200	12.7	0.000	2.2
	WB	2	0.1	3000	1500	240	9.5	0.011	2.8
Mobeen [53]	W-1	2.74	0.15	3283	1200	250	16	0.021	3.78
Han et al. [54]	W3	3	0.1	4500	1500	200	12.7	0.012	2
Liu [55]	W1	3.13	0.076	3750	1200	200	19.5	0.025	3
	W2	3.13	0.035	3750	1200	200	19.5	0.025	2.9
Ghorbani-Renani et al. [56]	A2C	2.08	0	2700	1300	200	25	0.027	3.18
Dazio et al. [8]	WSH1	2.28	0.051	4560	2000	150	10	0.012	1.04
	WSH2	2.28	0.057	4560	2000	150	10	0.012	1.38
	WSH3	2.28	0.058	4560	2000	150	12	0.011	2.03
	WSH4	2.28	0.057	4560	2000	150	12	0.000	1.6
	WSH5	2.28	0.128	4560	2000	150	8	0.013	1.36
	WSH6	2.26	0.108	4520	2000	150	12	0.017	2.07
Tran [57]	S63	2	0.073	2438	1219	152	19.1	0.018	3
	W1	2.03	0	1500	740	100	10	0.080	2.99
	W7	2	0	1500	750	125	10	0.000	3.48
	W9	2	0	1500	750	125	12	0.000	2.97
Christidis et al. [58]	W11	2	0	1500	750	125	12	0.000	3
Villalobos [59]	W-MC-C	2.175	0.1	3314.7	1524	203.2	25.4	0.013	3
	W-MC-N	2.175	0.1	3314.7	1524	203	25.4	0.008	2.5
Hube et al. [60]	W4	2.5	0.15	1750	700	75	10	0.008	1.6
Christidis et al. [61]	W13	2	0	1500	750	125	12	0.002	1.7
Lu et al. [62]	C1	2	0.035	2800	1400	150	10	0.004	2.6
	C2	4	0.035	5600	1400	150	10	0.004	2.5
	C3	6	0.035	8400	1400	150	10	0.004	2.6
	C4	2	0	2800	1400	150	10	0.000	1.5
	C5	2	0.066	2800	1400	150	10	0.008	2.5
	C6	4	0.035	5600	1400	150	10	0.012	2.5
Zhu & Guo [63]	MW	2.04	0.08	3460	1700	200	16	0.012	2.95
Abdulridha & Palermo [64]	W1-SR	2.4	0	2400	1000	150	11.3	0.038	4.07
Zhi et al. [65]	SW1-1	2.07	0.054	3312	1600	200	14	0.009	2.23
	SW2-1	2.08	0.063	3536	1700	200	16	0.013	2.6

Shegay et al. [66]	C10	4.6	0.092	10350	2250	200	16	0.015	3.8
	A10	4.6	0.092	10350	2250	200	16	0.013	3.7
	A14	4.6	0.14	10350	2250	200	16	0.017	3.1
	A20	4.6	0.21	10350	2250	200	16	0.019	2.7
Dashti et al. [14]	RWB	3	0.042	6000	2000	125	12	0.025	2
	RWT	3	0.047	6000	2000	135	12	0.023	2
	RWL	3.75	0.063	6000	1600	125	16	0.024	3
Lu et al. [18]	M1	4	0.035	5600	1400	150	10	0.012	2.5
	M2	4	0.035	5600	1400	150	12	0.012	3.5
	M3	4	0.035	5600	1400	150	12	0.012	2.5
	M4	4	0.035	5600	1400	150	16	0.012	3.5
Segura & Wallace [10]	WP1-1	3.74	0.1	8560	2286	152.4	15.9	0.018	2.02
	WP1-2	3.74	0.1	8560	2286	152.4	15.9	0.018	2.56
	WP2-1	3.74	0.1	8560	2286	152.4	15.9	0.029	2.16
	WP2-2	3.74	0.1	8560	2286	152.4	15.9	0.029	2.46
	WP3-1	3.74	0.1	8560	2286	152.4	15.9	0.021	2.1
	WP3-2	3.74	0.1	8560	2286	152.4	15.9	0.021	1.99
	WP6	3.57	0.1	8170	2286	191	15.9	0.025	4.08
	WP7	3.51	0.1	8030	2286	229	15.9	0.022	3.54
Yuan et al. [67]	SW-1	2	0.13	2560	1280	200	12	0.021	3.05
	SW-2	2	0.13	2560	1280	200	12	0.021	2.69
Zhu & Guo [68]	W-CIS	2.07	0.1	3525	1700	200	16	0.014	2.56
Tripathi et al. [16]	SWD-1	3	0.055	6000	2000	150	12	0.010	2.5
	SWD-2	3	0.055	6000	2000	150	12	0.008	2
	SWD-3	3	0.055	6000	2000	150	12	0.011	2.5
Niroomandi et al. [12]	SP1-Uni	3.75	0.046	6000	1600	125	16	0.015	2.5